Modeling the Effects of Drug Binding on the Dynamic Instability of Microtubules

Peter Hinow[1], Vahid Rezania[2], Manu Lopus[3], Mary Ann Jordan[3] and Jack A. Tuszyński[4]

[1]Department of Mathematical Sciences, University of Wisconsin – Milwaukee, P.O. Box 413, Milwaukee, WI 53201, USA

E-mail: hinow@uwm.edu

[2]Department of Physical Sciences, Grant MacEwan University, Edmonton AB, T5J 4S2, Canada

[3]Department of Molecular, Cellular, and Developmental Biology and the Neuroscience Research Institute, University of California, Santa Barbara, CA 93106, USA

[4]Cross Cancer Institute and Department of Physics, University of Alberta, Edmonton AB, T6G 2J1, Canada

Abstract.

We propose a stochastic model that accounts for the growth, catastrophe and rescue processes of steady state microtubules assembled from MAP-free tubulin in the possible presence of a microtubule associated drug. As an example for the latter, we both experimentally and theoretically study the perturbation of microtubule dynamic instability by S-methyl-D-DM1, a synthetic derivative of the microtubule-targeted agent maytansine and a potential anticancer agent. Our model predicts that among drugs that act locally at the microtubule tip, primary inhibition of the loss of GDP tubulin results in stronger damping of microtubule dynamics than inhibition of GTP tubulin addition. On the other hand, drugs whose action occurs in the interior of the microtubule need to be present in much higher concentrations to have visible effects.
Keywords: microtubules, dynamic instability, stochastic modeling

Submitted to: *Phys. Biol.*

PACS numbers: 87.10.Mn

1. Introduction

Microtubules are hollow and flexible cylindrical polymers of the protein tubulin that form a major component of the cytoskeleton of eukaryotic cells. They play a central role in maintenance of structural stability of the cell, intracellular vesicle transport and chromosome separation during mitosis. The polymerization of tubulin into microtubules and the subsequent catastrophic depolymerization have been studied extensively both experimentally and theoretically, see [1, 2, 3, 4, 5, 6, 7, 8, 9, 10, 11, 12, 13, 14] for just a few examples. The prevailing model to explain *dynamic instability*, the lateral cap model, is that a cap of GTP tubulin at the growing tip is required for stability of the polymer and that a loss of this GTP cap results in dramatic shortening of microtubules [15].

In the paper [14] we proposed a partial differential equation model inspired by dynamics of size-structured populations. The variables of that continuous model are length distributions of microtubules and the amounts of free tubulin. The major reactions are the polymerization of free GTP tubulin, the hydrolysis of assembled GTP tubulin to GDP tubulin, the decay and rescue of microtubules without a GTP cap and the recycling of free GDP tubulin to GTP tubulin. The model conserves the total amount of tubulin in all its forms. In addition, we allowed for the nucleation of fresh microtubules at certain specified (short) lengths. With a small number of parameters that have clear biochemical interpretations, we were able to reproduce commonly observed experimental behaviors, such as oscillations in the amount of tubulin assembled into microtubules. Obviously, the continuous model is not expected to reproduce the lengths of individual microtubules. To this end, in this paper we present a stochastic discrete model of microtubule dynamic instability and compare its predictions to observations of microtubule lengths from *in vitro* experiments that also include the presence of a dynamic instability suppressing drug.

Stochastic discrete models of biopolymer dynamics have been investigated, among others, in [4, 5, 16, 17, 18, 12, 13, 19, 20]. Bolterauer *et al.* [4, 5] introduced a stochastic model to study the dynamics of free microtubules using the master equation approach. They showed that in the continuum limit the microtubule length distribution follows a bell-shaped curve. Mishra *et al.* [20] applied a similar technique to elaborate the effect of catastrophe-suppressing drugs on the dynamic instability of microtubules. They assumed that drug molecules bind rapidly to free tubulin in the solution. Then, the drug-tubulin complexes bind to the growing tips of the microtubules and reduce the catastrophe frequency by stabilizing the microtubule caps. They also assumed that the drug-tubulin complex has a lower attachment rate than drug-free tubulin. As a result, one would expect to observe shorter drug-treated microtubules in the steady state. While they found a qualitative reduction in catastrophe frequency, surprisingly, they found that the drug-treated microtubules have the same length distribution as free microtubules.

Here we present a stochastic model that represents the same set of reactions as our

continuous model in [14], except for the nucleation of fresh microtubules which is an unnecessary complication for the case studied here. Similar to other stochastic models [16, 17, 12, 13, 19, 20], our underlying model that describes microtubule dynamics without drugs is based on an effective two-state model, switching between a growing and shortening state. As in [14] and in contrast to other works such as [16, 20], we couple the growth velocity of microtubules to the amount of free GTP tubulin and the model is constructed so as to preserve the total amount of tubulin in all its forms. Following [8], we include hydrolysis events of two kinds, namely *scalar hydrolysis* (conversion of bound GTP tubulin to GDP tubulin with equal probability) and *vectorial hydrolysis* (the probability is enhanced by a GDP tubulin neighbor). Furthermore, in contrast to previous models that simulate one microtubule at a time, we simulate several microtubules at the same time. This enables us to capture a more realistic situation similar to one in experiments. Last but not least, a great advantage of our model is that it can be implemented straightforwardly with the help of the Gillespie Algorithm [21], an exact simulation method for stochastic chemical reactions. Our goal is to explain individual length observations of microtubules growing without microtubule associated proteins (MAPs) *in vitro* or length constraints (as in [17]). Moreover, we investigate the effects of tubulin-binding drugs on microtubule dynamic instability. These drugs belong roughly to one of two classes, namely those that bind to assembled microtubules and those that bind to free tubulin [22]. This difference in behaviors may be due to conformational changes of the α/β-tubulin heterodimer [23] (the tubulin *unit* from now on) upon incorporation into the microtubule lattice that expose or hide the binding site for the drug molecule. Apart from these different binding modes, the effects on the microtubule reactions can also differ [24]. Some drugs mainly slow down microtubule formation while others mainly prevent microtubule decay. This is not a strict dichotomy in that some drugs can have multiple actions, depending on their concentration. For example, vinblastine inhibits microtubule formation at high drug concentrations, and inhibits microtubule decay at low concentrations [22]. Moreover, there are multiple action mechanisms of drugs, for example either by preventing addition of GTP tubulin,loss of GDP tubulin from an exposed tip or by preventing the hydrolysis of GTP tubulin incorporated in the microtubule. In any case, within a living cell exposed to anti-mitotic agents, mitosis cannot be completed and the cell dies. This property of tubulin-binding drugs leads to many successful anti-cancer chemotherapeutics such as paclitaxel, vincristine, vinblastine to name but a few. Maytansine and its derivatives are known to suppress microtubule dynamics *in vitro* and in cells [25]. As an example, we focus on the potential anticancer agent S-methyl-D-DM1, a synthetic derivative of the microtubule-binding agent maytansine. Antibody-DM1 conjugates are currently under clinical trials with promising results [26]. In our model, drugs act by decelerating (or accelerating) binding or release reactions by a certain factor. Thus the strength of the action can be quantified and linked to the binding energy through the standard Arrhenius relation.

2. The stochastic model

We consider a linear model of the microtubule and disregard the fact that it actually consists of 13-17 protofilaments arranged in a helical lattice. Tubulin can be added to the microtubule in form of small oligomers of varying sizes [27].

Let $m \geq 1$ be the number of dynamic microtubules. The state of each microtubule is represented as a word $\boldsymbol{v}^k = (\ldots, v_2^k, v_1^k, v_0^k)$, $k = 1, \ldots, m$ on the binary alphabet $\{0, 1\}$ where the letter 1 stands for a position occupied by a GTP tubulin unit and 0 stands for a position occupied by a GDP tubulin unit. The length of the microtubule $\boldsymbol{v}^k$ is denoted by $|\boldsymbol{v}^k|$. The number of GTP tubulin units within $\boldsymbol{v}^k$ is denoted by $I(\boldsymbol{v}^k)$. The "tip" of the microtubule is the letter v_0^k and this is the only position where growth or shrinkage can occur. Consecutive strings of 0s and 1s are called GDP zones and GTP zones, respectively. The number of boundaries between such zones is denoted by $B(\boldsymbol{v}^k)$. The numbers of free GTP tubulin and GDP tubulin are denoted by N^T and N^D, respectively. These numbers can be converted to and from concentrations, if the volume in which the reactions take place is given. The following reactions occur (see also Figure 1).

(i) Growth by attachment of GTP tubulin(s)

$$\boldsymbol{v}^k \mapsto [\boldsymbol{v}^k \underbrace{1 \ldots 1}_{l}], \quad N^T \mapsto N^T - l,$$

at rate (derived from mass action kinetics)

$$\lambda N^T (v_0^k + p(1 - v_0^k)). \tag{1}$$

Notice that every microtubule has its own growth reaction so that there are m of them. The number of added GTP tubulin units l can be set to a fixed value (say, 1) or drawn from a Poisson distribution with parameter L. The dimensionless parameter $p \geq 0$ is the propensity of a rescue event when a GDP tubulin unit at the tip of the microtubule is exposed. In the simplest case, $p = 1$, attachment of a new GTP tubulin is independent of the tip status.

(ii) Loss of a GDP tubulin (when the tip is in the state 0)

$$\boldsymbol{v}^k \mapsto (\ldots, v_2^k, v_1^k), \quad N^D \mapsto N^D + 1,$$

at rate $\mu_{GDP}(1 - v_0^k)$. Again there are m such shrinking reactions.

(iii) Loss of a GTP tubulin (when the tip is in the state 1)

$$\boldsymbol{v}^k \mapsto (\ldots, v_2^k, v_1^k), \quad N^T \mapsto N^T + 1,$$

at rate $\mu_{GTP} v_0^k$.

(iv) Hydrolytic conversion of a bound GTP tubulin $\boldsymbol{v}^{k^*} \mapsto \widetilde{\boldsymbol{v}}^{k^*}$ at rate $\delta_{sc} \sum_{k=1}^m I(\boldsymbol{v}^k)$. The index k^* is chosen uniformly in the set $\{1, \ldots, m\}$ and a random position of $\boldsymbol{v}^{k^*}$ that is occupied by 1 is changed to 0 (this hydrolysis mechanism is called *scalar* hydrolysis in [8]).

(v) Hydrolytic conversion of a bound GTP tubulin $\boldsymbol{v}^{k^*} \mapsto \widetilde{\boldsymbol{v}}^{k^*}$ at rate $\delta_{vec} \sum_{k=1}^{m} B(\boldsymbol{v}^k)$. Again, the index k^* is chosen uniformly in the set $\{1, \ldots, m\}$ and the word $\widetilde{\boldsymbol{v}}^{k^*}$ is created by selecting randomly a position of $\boldsymbol{v}^{k^*}$ where a 1 neighbors a 0 and changing that 1 to 0 (this hydrolysis mechanism is called *vectorial* hydrolysis in [8], see Figure 2, left panel).

(vi) Recycling of free GDP tubulin to GTP tubulin

$$N^D \mapsto N^D - 1, \quad N^T \mapsto N^T + 1,$$

at rate κN^D. It is assumed that a sufficient amount of chemical energy in the form of free GTP is always present.

This scheme can be simplified by setting some parameter values to zero. For example, one may disregard the possibility of a bound GTP tubulin to be lost again ($\mu_{GTP} = 0$, cf. [8]), although other authors argue that this may take place in up to 90% of all binding events [28]. The addition size l can be selected to be constant 1. The hydrolysis reaction (iv) picks any bound GTP tubulin and changes it to a GDP tubulin, thereby creating islands of GTP tubulin within the length of the microtubule. That this is possible and important for the rescue process was recently shown by Dimitrov *et al.* [29]. Both hydrolysis mechanisms in concert provide an indirect coupling of the hydrolysis reaction to the addition of new GTP tubulin units [8].

Tubulin-binding drugs can bind to tubulin in one of two states, whether it is free or bound within a microtubule. Here, we consider drugs that suppress microtubule dynamic instability by specifically binding to microtubules. For every microtubule encoded by a word $\boldsymbol{v}$, we introduce a second word $\boldsymbol{w} = (\ldots, w_2, w_1, w_0)$ over the alphabet $\{0, 1\}$ (the drug state), of equal length as $\boldsymbol{v}$. Here $w_i = 1$, if the tubulin unit at position v_i is occupied by a drug molecule and $w_i = 0$ otherwise. There are binding events of drug molecules to unoccupied sites and release of drug molecules from the microtubule. Let $E(\boldsymbol{w})$ be the number of available sites for drug binding and let $F(\boldsymbol{w})$ be the number of drug occupied sites. The latter is always the sum of the entries 1 in $\boldsymbol{w}$ while the former may be only a subset of entries 0 in $\boldsymbol{w}$. We have the association and dissociation events

(vii) Binding of drug to tubulin units within the microtubule

$$\boldsymbol{w}^{k^*} \mapsto \widetilde{\boldsymbol{w}}^{k^*}, \quad D \mapsto D - 1,$$

at rate $\rho D \sum_{k=1}^{m} E(\boldsymbol{w}^k)$. The new word $\widetilde{\boldsymbol{w}}^{k^*}$ is obtained by selecting randomly one letter 0 among the sites available for binding and changing it to 1. This set may be the set of all entries 0 or the entries 0 that are within a certain distance from the tips or the unoccupied tips alone.

(viii) Release of drug from the occupied sites of the microtubule

$$\boldsymbol{w}^{k^*} \mapsto \widetilde{\boldsymbol{w}}^{k^*}, \quad D \mapsto D + 1,$$

at rate $\sigma \sum_{k=1}^{m} F(\boldsymbol{w}^k)$. The new word $\widetilde{\boldsymbol{w}}^{k^*}$ is obtained by changing one randomly selected letter 1 in any of the drug words to 0.

The reactions (i)–(vi) have the same outcomes as far as changes in numerical quantities are concerned, however the rates of reactions (i), (ii) and (iii) have a more complicated dependence upon the status of the microtubule tip. Since the tip can now have four different states, the attachment process (i) to microtubule k occurs at rate

$$\lambda N^T \left((v_0^k + p(1-v_0^k))(1-w_0^k) + r(v_0^k + p(1-v_0^k))w_0^k\right), \tag{2}$$

where the dimensionless non-negative constant r modulates the attachment propensity compared to the drug-free tip, see Equation (1). Small values of r would mean that attachment of new GTP tubulin units is hindered by drug molecules bound to the tip. On the other hand, values $r > 1$ would increase microtubule polymerization. The shrinking reactions (ii) and (iii) occur at rates

$$\mu_{GDP}(1-v_0^k)((1-w_0^k) + qw_0^k), \quad \text{and} \quad \mu_{GTP}v_0^k((1-w_0^k) + qw_0^k), \tag{3}$$

where a small value of $q \geq 0$ implies a high level of protection afforded by a drug molecule bound to the tip. If a drug bound tubulin can fall off a microtubule (i.e. if $q > 0$), then the drug-tubulin compound is assumed to dissociate immediately. We refer to Figure 1 for the possible interactions of the drug with the microtubules (as implemented in this paper).

There are also possible drug actions beyond the microtubule tips. As was first discovered by Lin and Hamel [30], a drug can also inhibit the hydrolysis of bound GTP tubulin. This can be implemented by "splitting" the scalar and vectorial hydrolysis reactions (iv) and (v). More precisely, let $I_0(\boldsymbol{v}^k)$ and $I_1(\boldsymbol{v}^k)$ be the number of GTP tubulin units within the microtubule word $\boldsymbol{v}^k$ that are unoccupied respectively occupied by a drug molecule. Then the scalar hydrolysis reactions (iv^0) and (iv^1) occur at rates $\delta_{sc}\sum_{k=1}^m I_0(\boldsymbol{v}^k)$ (as before) and $s\delta_{sc}\sum_{k=1}^m I_1(\boldsymbol{v}^k)$ (with $0 \leq s \leq 1$). A similar splitting is used for the vectorial hydrolysis reaction (v).

3. Materials and Methods

Tubulin ($15\,\mu M$), phosphocellulose purified, MAP-free, was assembled on the ends of sea urchin (*Strongylocentrotus purpuratus*) axoneme fragments at $30°C$ in $87\,mmol/L$ Pipes, $36\,mmol/L$ Mes, $1.4\,mmol/L$ $MgCl_2$, $1\,mmol/L$ EGTA, pH 6.8 (PMME buffer) containing $2\,mmol/L$ GTP for 30 *min* to achieve steady state. We used a $100\,nmol/L$ concentration of S-methyl-D-DM1 ($N^{2'}$-deacetyl-$N^{2'}$-(3-thiomethyl-1-oxopropyl)-D-maytansine [31], see Figure 2, right panel), which had no considerable effect on microtubule polymer mass, to analyze their individual effects on dynamic instability. Time-lapse images of microtubule plus ends were obtained at $30°C$ by video-enhanced differential interference contrast microscopy at a spatial resolution of $0.3\,\mu m$ using an Olympus IX71 inverted microscope with a 100 × oil immersion objective (NA = 1.4). The end of an axoneme that possesses more, faster growing, and longer microtubules than the other end was designated as the plus end as described previously [32, 33]. Microtubule dynamics were recorded for 40 *min* at $30°C$, capturing $\sim 10\,min$ long videos for each area under observation. The microtubules were tracked

approximately every 3 s using RTMII software, and the life-history data were obtained using IgorPro software (MediaCybernetics, Bethesda, MD) [34].

We have programmed the reactions (i)–(viii) using the Gillespie Algorithm [21] (in JAVA, available from the corresponding author upon request). This algorithm simulates the chemical reactions as collisions of particles in real time and its parameters are the actual reaction rates, not probabilities. If the empty word is reached, then a new microtubule is created (a word containing a single GTP tubulin unit). The gain in length due to addition of a single tubulin unit is taken to be $\ell = 8\,nm/13 = 0.6\,nm$; see e.g. [8, Equation (2)].

4. Results

Results of the *in vitro* experiments are shown in Figures 3 and 7. During periods of growth, the untreated microtubules grow at a velocity of $\approx 3\,\mu m\,min^{-1}$ while during periods of shrinkage, microtubules shrink at $\approx 20\,\mu m\,min^{-1}$. While they are infrequent, we attribute occasional periods of stagnation to the spatial resolution of the microscope of approximately 400 tubulin dimer units.

The left panels of Figures 4, 5 and 6 show possible simulations of the control scenario in the absence of drugs. The choice of appropriate parameter values for the simulations is a difficult problem, since different values have been reported in different literature sources and some parameters have only been estimated on the basis of the Arrhenius Equation (see [14, Table 1] for some ranges). While there is no unique choice of parameter values, we observe a good agreement of the simulated and observed growth and shrinking velocities, for the choice of parameter values in Table 1, see Figure 4. To quantify the agreement between the simulations and the experimental data we used the absolute Fourier spectra [35] of the length time series. We first re-sampled both the experimental data and the numerical simulations on equispaced time grids at approximately $0.4\,Hz$. In order to make different simulations comparable, we subtracted the mean from each length time series so that the resulting normalized lengths have mean zero. If l_n, $n = 0, \ldots, N-1$ are the re-sampled normalized lengths, then the discrete Fourier transform is given by the absolute values of

$$L_k = \sum_{n=0}^{N-1} l_n \exp\left(-\frac{2\pi i k n}{N}\right), \quad k = 0, \ldots, N-1.$$

This is conveniently done with the help of the fast Fourier transform routine `fft` in SCILAB‡. Results are shown in the right panels of Figures 3 and 4, showing a good agreement among experimental and simulated data of the location and the height of the peak of the averaged spectra. In Figure 6, a sensitivity check is run with significantly larger parameter values $\lambda = 1.0\,(\ell s)^{-1}$, $\mu_{GDP} = 2000\,s^{-1}$, $\delta_{sc} = \delta_{vec} = 3.0\,(\ell s)^{-1}$ and $\kappa = 0.5\,s^{-1}$, see Table 1 for comparison. As a result, higher oscillation frequencies would be expected in the Fourier spectra due to higher rate of polymerization,

‡ Open source software; available at `www.scilab.org`.

depolymerization, hydrolysis and recycling events. This is clearly shown in the right panel of Figure 6, as the spectrum visibly shifts towards higher frequencies.

The presence of the drug clearly decelerates the dynamic activity of the microtubules as can be seen from Figure 7. This is also visible in the reduced peak heights of the Fourier spectra, while the position of the peak, i.e. the main frequency of the oscillations remains unchanged, at least not discernible on the $0.4\,Hz$ frequency grid, see also Figure 9. With the same parameter values as in the control in Figure 4, we simulated the presence of a microtubule-binding drug that suppresses strongly the addition of new GTP tubulin ($r = 0.01$), completely inhibits the loss of tubulin at the tip ($q = 0$) and does not affect the hydrolysis of bound GTP tubulin ($s = 1$). The open drug binding sites are all entries 0 in the drug words. The results are shown in Figure 8. There are 400 drug molecules present in the simulation (compared to $\approx 10^5$ tubulin units). This amount of roughly 100 drug molecules per microtubule matches approximately the concentration of S-methyl-D-DM1 in the experiments.

The nonlocal drug action mechanism where the bound drug inhibits hydrolysis of GTP tubulin is much less effective in suppressing microtubule dynamic instability. In Figure 10 we show simulations of 5 microtubules built of approximately 10^5 tubulin units in the presence of a drug that completely inhibits hydrolysis reactions (iv) and (v), i.e. $s = 0$ without affecting the binding and loss reactions, $r = q = 1$. We observe that a much higher amount of drug, namely of the order of tubulin units, is required to have any visible effect, while at the same time, long periods of shortening still occur.

In order to better understand the influence of a drug acting at the microtubule tip, we systematically varied the parameters r and q, keeping all other parameters and the drug concentration constant. We consider the reduction of the peak height of the absolute Fourier spectra relative to the control scenario. If the drug molecules are free to bind any of the open drug binding sites, then a complete repression of the loss reactions (ii) and (iii), i.e. $q = 0$ is required to efficiently suppress the dynamic instability of microtubules, see Figure 11, left panel. An alternative is to allow drug molecules to bind only at the tip [33]. In that case, the suppression effect persists for weaker drug effects (Figure 11, right panel). However, it is still more important to suppress the loss reactions (small value of q) than to suppress the growth reaction ($r \approx 1$ is admissible). Notice that these predictions of the model are drawn from the shapes of the surfaces in Figure 11, not from particular values.

5. Discussion

Spatial and temporal regulation of the dynamic instability of microtubules is essential to carry out several vital cellular functions. In cells, the dynamicity of microtubules is regulated by a number of proteins such as MAPs [11], G proteins [36], and the plus end tracking proteins, including EB1 [11]. Perturbations in the innate dynamicity of microtubules induce cell cycle arrest and thereby inhibit cell proliferation. Thus, compounds that target microtubules are potential anticancer drugs. Our recent studies

have found synthetic derivatives of maytansine such as DM1 (for drug maytansinoid 1) that can be conjugated to tumor-specific antibodies as potent suppressors of microtubule dynamics [25, 33]. Antibody-DM1 Conjugates are under clinical evaluation, and they show promising early results. Thus, the synthetic derivative of maytansine S-methyl-D-DM1 is a good example to complement our modeling studies.

In this paper we have presented a detailed reaction scheme for microtubule polymerization, GTP tubulin hydrolysis, catastrophic shrinking, recycling and interaction with tubulin-binding drugs. Our *in silico* simulations show good agreement of Fourier spectra with experimental data of growing microtubules under control conditions and treated with the maytansine derivative S-methyl-D-DM1. Our model allows to accommodate a wide variety of drug binding mechanisms and interactions of the drug with the normal microtubule polymerization and depolymerization processes. We find that drugs that act at the microtubule tip by inhibiting addition of GTP tubulin and loss of GDP tubulin are effective suppressors of microtubule dynamic instability. This would also be the action mechanism of S-methyl-D-DM1. Among these two actions, the inhibition of the loss of GDP tubulin is more important than the inhibition of the growth reaction. A localized binding to the tip inhibits dynamic instability even more. On the other hand, drugs whose action is to inhibit hydrolysis of bound GTP tubulin need to be present at numbers comparable to the number of tubulin units to have a visible effect on microtubule dynamic instability.

Our assumption in modeling the drug binding reaction (vii) has been that either the drug molecule binds to any open binding site with equal probability or that it binds only at an open site at the tip. The former is the binding mode of a drug like paclitaxel that stabilizes a microtubule along its entire length. Other drugs, such as vinblastine bind with high affinity only at the microtubule plus end [22]. In future work we will implement a probability of drug binding that decreases with increasing distance from the tip.

It is well known that some drugs have different effects at different concentrations. For example, taxol (paclitaxel) increases microtubule polymerization at high concentrations (50 taxol molecules per 100 tubulin molecules), while it reduces the rate of shortening at low concentrations (1 taxol molecule per 100 tubulin molecules) [22]. This suggests the need for a "nonlocal" generalization of the perturbation of the binding and shrinking processes, in contrast to the present choices in Equations (2) and (3).

The design of therapeutic drugs requires long and tedious searches among all possible binding sites on the target. Identifying the most favorable binding site (with the lowest binding energy), however, is needed to design or discover a drug compound with the highest possible efficacy. Information on drug-ligand binding affinities (for tubulin and tubulin-binding drugs in particular) can be extracted by careful comparison of simulation results and experimental data. Such estimations of binding energies will be addressed in a future study.

Acknowledgments

Part of this research was carried out during visits at the University of Wisconsin – Milwaukee and the University of Alberta, Edmonton. We thank our respective institutions for their warm hospitality. PH is partially supported by NSF grant DMS-1016214. Financial support was partially supplied by grants from NSERC, Alberta's Advanced Education and Technology, the Allard Foundation and the Alberta Cancer Foundation to JAT and from grant NIH CA57291 and a gift from ImmunoGen Inc. to MAJ. We thank Dr. Ravi Chari (ImmunoGen Inc., Waltham, MA) for providing us with the drug S-methyl-D-DM1 and Bruce Fenske and Philip Winter (University of Alberta) for implementing the Gillespie algorithm. We are much indebted to two anonymous readers whose comments greatly helped to improve the paper.

References

[1] Jackson, M. B. and S. A. Berkovitz. Nucleation and the kinetics of microtubule assembly. *Proc. Natl. Acad. Sci. USA*, **77**:7302–7305, 1980.

[2] Mandelkow, E., E. M. Mandelkow, H. Hotani, B. Hess, and S. C. Müller. Spatial patterns from oscillating microtubules. *Science*, **246**:1291–1293, 1989.

[3] Walker, R. A., E. T. O'Brien, N. K. Pryer, M. E. Soboeiro, W. A. Voter, H. P. Erickson, and E. D. Salmon. Dynamic instability of individual microtubules analyzed by video light microscopy: rate constants and transition frequencies. *J. Cell Biol.*, **107**:1437–1448, 1988.

[4] Bolterauer, H., H.–J. Limbach, and J. A. Tuszyński. Microtubules: strange polymers inside the cell. *Bioelectrochem. Bioenerg.*, **48**:285–295, 1999.

[5] Bolterauer, H., H.–J. Limbach, and J. A. Tuszyński. Models of assembly and disassembly of individual microtubules: stochastic and averaged equations. *J. Biol. Phys.*, **25**:1–22, 1999.

[6] Mitchison, T. and M. Kirschner. Dynamic instability of microtubule growth. *Nature*, **312**:237–242, 1984.

[7] Flyvbjerg, H., T. E. Holy, and S. Leibler. Stochastic dynamics of microtubules: A model for caps and catastrophes. *Phys. Rev. Lett.*, **73**:2372 –2375, 1994.

[8] Flyvbjerg, H., T. E. Holy, and S. Leibler. Microtubule dynamics: caps, catastrophes, and coupled hydrolysis. *Phys. Rev. E*, **54**:5538–5560, 1996.

[9] Jobs, E., D. E. Wolf, and H. Flyvbjerg. Modeling microtubule oscillations. *Phys. Rev. Lett.*, **79**:519–522, 1997.

[10] Rezania, V., O. Azarenko, M. A. Jordan, H. Bolterauer, R. F. Ludueña, J. T. Huzil, and J. A. Tuszyński. Microtubule assembly of isotypically purified tubulin and its mixtures. *Biophys. J.*, **95**:1–16, 2008.

[11] Lopus, M., M. Yenjerla, and L. Wilson. *Microtubule Dynamics*, volume **3** of *Wiley Encyclopedia of Chemical Biology*, pages 153–160. 2009.

[12] van Buren, V., D. J. Odde, and L. Cassimeris. Estimates of lateral and longitudinal bond energies within the microtubule lattice. *Proc. Natl. Acad. Sci. USA*, **99**:6035–6040, 2002.

[13] van Buren, V., L. Cassimeris, and D. J. Odde. Mechanochemical model of microtubule structure and self-assembly kinetics. *Biophys. J.*, **89**:2911–2926, 2005.

[14] Hinow, P., V. Rezania, and J. A. Tuszyński. A continuous model for microtubule dynamics with collapse, rescue and nucleation. *Phys. Rev. E*, **80**:031904, 2009. arXiv:0811.2245.

[15] Bayley, P. M., M. J. Schilstra, and S. R. Martin. A lateral cap model of microtubule dynamic instability. *FEBS Letters*, **259**:181–184, 1989.

[16] Antal, T., P. L. Krapivsky, S. Redner, M. Mailman, and B. Chakraborty. Dynamics of an idealized model of microtubule growth and catastrophe. *Phys. Rev. E*, **76**:041907, 2007. arXiv:q-bio/0703001.

[17] Gregoretti, I. V., G. Margolin, M. S. Alber, and H. V. Goodson. Insights into cytoskeletal behavior from computational modeling of dynamic microtubules in a cell–like environment. *J. Cell Sci.*, **119**:4781–4788, 2006. arXiv:q-bio/0604023.

[18] Matzavinos, A. and H. G. Othmer. A stochastic analysis of actin polymerization in the presence of twinfilin and gelsolin. *J. Theor. Biol.*, **249**:723–736, 2007.

[19] Brun, L., B. Rupp, J. Ward, and F. Nedelec. A theory of microtubule catastrophes and their regulation. *Proc. Natl. Acad. Sci. USA*, **106**:21173–21178, 2009.

[20] Mishra, P. K., A. Kunwar, S. Mukherji, and D. Chowdhury. Dynamic instability of microtubules: Effect of catastrophe-suppressing drugs. *Phys. Rev. E*, **72**:051914, 2005. arXiv:cond-mat/0310546.

[21] Gillespie, D. T. Exact stochastic simulation of coupled chemical reactions. *J. Phys. Chem.*, **81**:2340–2361, 1977.

[22] Jordan, M. A. and K. Kamath. How do microtubule-targeted drugs work? An overview. *Current Cancer Drug Targets*, **7**:730–742, 2007.

[23] Bennett, M. J., J. K. Chik, G. W. Slysz, T. Luchko, J. A. Tuszyński, D. L. Sackett, and D. C. Schriemer. Structural mass spectrometry of the $\alpha\beta$-tubulin dimer supports a revised model of microtubule assembly. *Biochemistry*, **48**:4858–4870, 2009.

[24] Correia, J. J. and S. Lobert. Molecular mechanisms of microtubule acting cancer drugs. In T. Fojo, editor, *Microtubules in Health and Disease*, pages 21–46. 2008.

[25] Oroudjev, E., M. Lopus, L. Wilson, C. Audette, C. Provenzano, H. Erickson, Y. Kovtun, R. Chari, and M. A. Jordan. Maytansinoid-antibody conjugates induce mitotic arrest by suppressing microtubule dynamic instability. *Mol. Cancer Therapeutics*, **9**:2700–2713, 2010. doi:10.1158/1535-7163.MCT-10-0645.

[26] Lopus, M. Antibody-DM1 conjugates as cancer therapeutics. *Cancer Lett.*, **307**:113–118, 2011.

[27] Mozziconacci, J., L. Sandblad, M. Wachsmuth, D. Brunner, and E. Karsenti. Tubulin dimers oligomerize before their incorporation into microtubules. *PLoS ONE*, **3**:e3821, 2008.

[28] Howard, J. and A. A. Hyman. Growth, fluctuation and switching at microtubule plus ends. *Nat. Rev. Mol. Cell Biol.*, **10**:569–574, 2009.

[29] Dimitrov, A., M. Quesnoit, S. Moutel, I. Cantaloube, C. Poüs, and F. Perez. Detection of GTP-Tubulin conformation in vivo reveals a role for GTP remnants in microtubule rescues. *Science*, **322**:1353–1356, 2008.

[30] Lin, C. M. and E. Hamel. Effects of inhibitors of tubulin polymerization on GTP hydrolysis. *J. Biol. Chem.*, **256**:9242–9245, 1981.

[31] Widdison, W. C., S. D. Wilhelm, E. E. Cavanagh, K. R. Whiteman, B. A. Leece, Y. Kovtun, V. S. Goldmacher, H. Xie, R. M. Steeves, R. J. Lutz, R. Zhao, L. Wang, W. A. Blättler, and R. V. J. Chari. Semisynthetic maytansine analogues for the targeted treatment of cancer. *J. Med. Chem.*, **49**:4392–4408, 2006.

[32] Yenjerla, M., M. Lopus, and L. Wilson. *Analysis of Dynamic Instability of Steady-State Microtubules In Vitro by Video-Enhanced Differential Interference Contrast Microscopy*, volume **95** of *Methods in Cell Biology*, chapter 11, pages 189–206. 2010.

[33] Lopus, M., E. Oroudjev, L. Wilson, S. Wilhelm, W. Widdison, R. Chari, and M. A. Jordan. Maytansine and cellular metabolites of antibody-maytansinoid conjugates strongly suppress microtubule dynamics by binding to microtubules. *Mol. Cancer Therapeutics*, **9**:2689–2699, 2010. doi:10.1158/1535-7163.MCT-10-0644.

[34] Yenjerla, M., N. E. LaPointe, M. Lopus, C. Cox, M. A. Jordan, S. C. Feinstein, and L. Wilson. The neuroprotective peptide NAP does not directly affect polymerization or dynamics of reconstituted neural microtubules. *J. Alzheimer Dis.*, **19**:1377–1386, 2010.

[35] Odde, D. J., H. M. Buettner, and L. Cassimeris. Spectral analysis of microtubule assembly

dynamics. *AIChE Journal*, **42**:1434–1442, 1996.

[36] Davé, R. H., W. Saengsawang, S. Davé, M. Lopus, L. Wilson, and M. M. Rasenick. A molecular and structural mechanism for G-protein mediated microtubule destabilization. *J. Biol. Chem*, **286**:4319–4328, 2011.

[37] Carlier, M. F., R. Melki, D. Pantaloni, T. L. Hill, and Y. Chen. Synchronous oscillations in microtubule polymerization. *Proc. Natl. Acad. Sci. USA*, **84**:5257, 1987.

6. Tables and Figures

parameter	value	remark	reference
λ	$0.4\,(\ell s)^{-1}$	addition rate of GTP tubulin to GTP tip	[16]
p	0.05	reduction of GTP addition to GDP tip	[16]
μ_{GDP}	$800\,s^{-1}$	loss of GDP tubulin from tip	[3]
μ_{GTP}	$1.5\,s^{-1}$	loss of GTP tubulin from tip	[8, 28]
δ_{sc}	$1.2\,(\ell s)^{-1}$	rate of scalar hydrolysis	[8]
δ_{vec}	$1.2\,(\ell s)^{-1}$	rate of vectorial hydrolysis	[8]
κ	$0.1\,s^{-1}$	rate of GDP tubulin recycling	[37]
L	6	average GTP tubulin addition size	[27]
ρ	$1.0 s^{-1}$	rate of drug binding	
σ	$0.1\,s^{-1}$	rate of drug release	

Table 1. Baseline values of parameters used in the stochastic simulations. Here $\ell = 0.6\,nm$ is the gain in length by addition of a single tubulin unit. The references provide further discussion and sometimes comparable values.

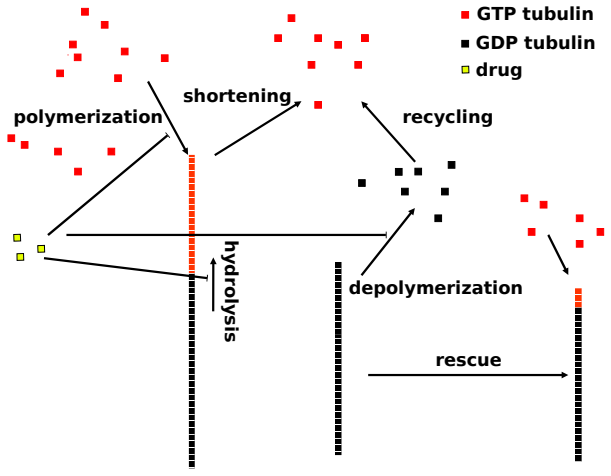

Figure 1. The reactions and possible drug interactions implemented in our stochastic model. A drug may also promote polymerization and depolymerization.

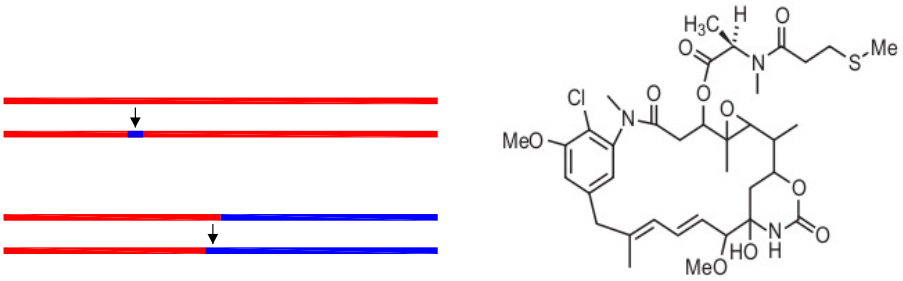

Figure 2. (Left panel) Schematic depiction of the two hydrolysis mechanisms. The scalar hydrolysis reaction (p. 4 (iv), top) picks a random bound GTP tubulin and changes it into a bound GDP tubulin. The vectorial hydrolysis reaction (p. 5 (v), bottom) occurs at a boundary between a GDP zone and a GTP zone. (Right panel) Structural formula of the maytansine analog S-methyl-D-DM1.

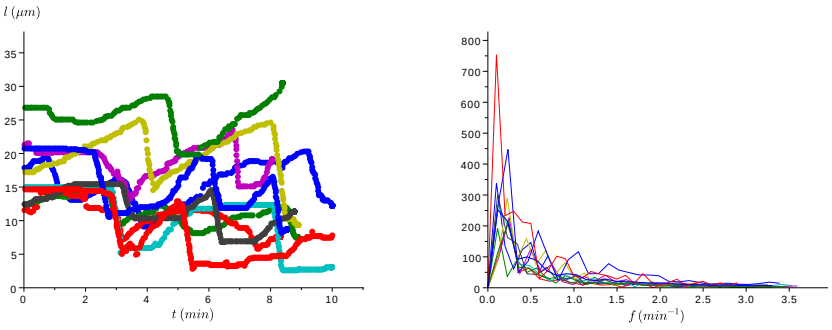

Figure 3. (Left panel) Length time series of 10 microtubules in absence of drug. Notice that life histories from several experiments are plotted in the same diagram. (Right panel) Absolute Fourier spectra of the control experimental data that were normalized to mean length zero. The thick blue line is the average of the 10 individual spectra.

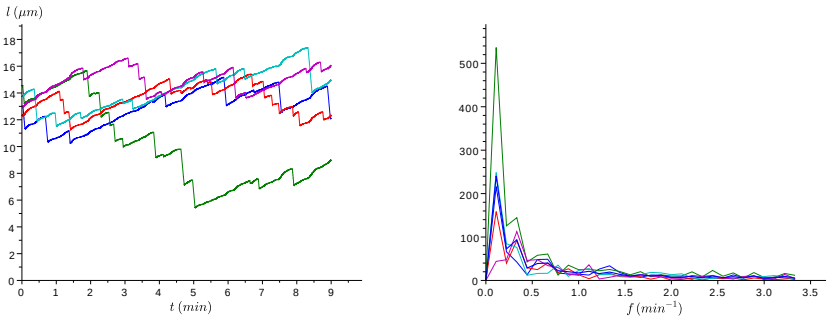

Figure 4. (Left panel) Simulation of $m = 5$ microtubules starting from random initial states, with a total of $\approx 10^5$ tubulin units. The parameter values are as in Table 1. GTP tubulin is added in the form of oligomers whose length is Poisson distributed with with mean $L = 6$. The resulting average growth velocity during periods of growth is approximately $2\,\mu m\,min^{-1}$ while the resulting shrinking velocity is approximately $20\,\mu m\,min^{-1}$. (Right panel) Absolute Fourier spectra of the simulation data, normalized to mean length zero. The thick blue line is the average of the 5 individual spectra.

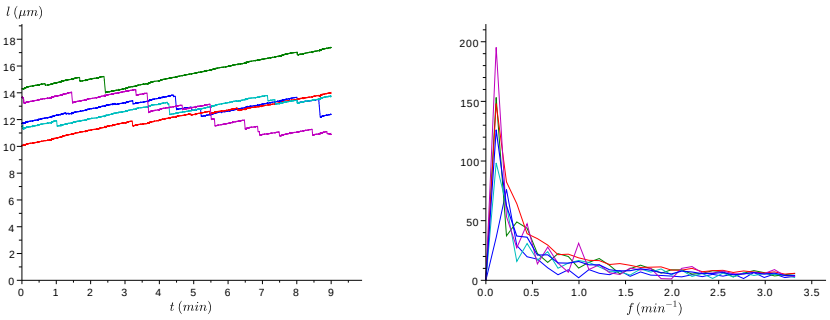

Figure 5. (Left panel) Simulation of $m = 5$ microtubules with parameter values as in Table 1 and Figure 4 except that GTP tubulin is added in units of fixed length $L = 1$. (Right panel) Absolute Fourier spectra of the simulation data, normalized to mean length zero and their average.

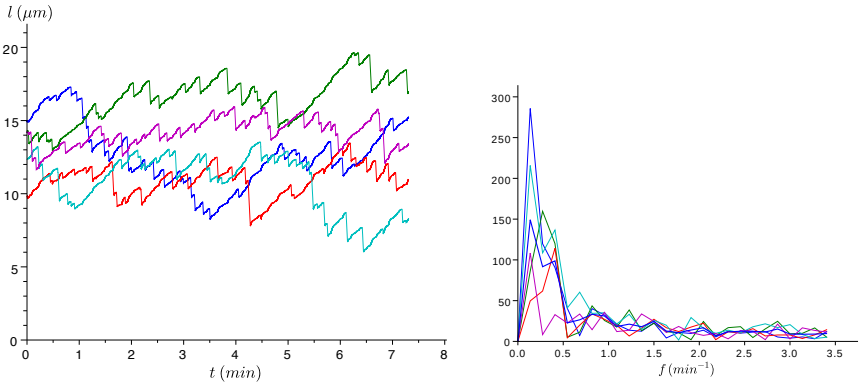

Figure 6. (Left panel) Simulation of $m = 5$ microtubules with parameter values $\lambda = 1.0\,(\ell s)^{-1}$, $\mu_{GDP} = 2000\,s^{-1}$, $\delta_{sc} = \delta_{vec} = 3.0\,(\ell s)^{-1}$ and $\kappa = 0.5\,s^{-1}$, all of which are larger than those in Table 1. (Right panel) The corresponding absolute Fourier spectra show a visible shift towards higher frequencies.

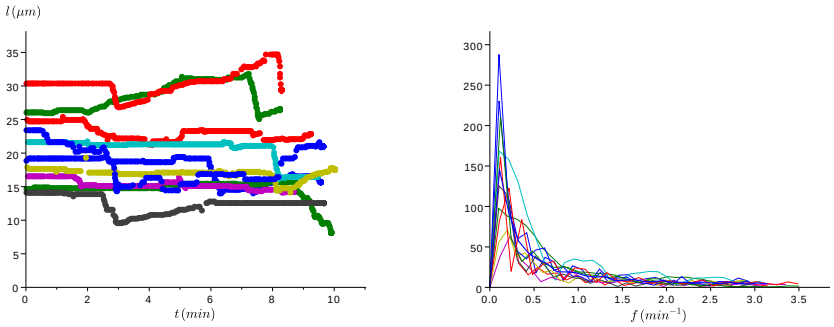

Figure 7. (Left panel) Length time series of 10 microtubules in presence of the drug S-methyl-D-DM1. (Right panel) The corresponding absolute Fourier spectra, normalized to mean length zero. The thick blue line is the average of the 10 individual spectra.

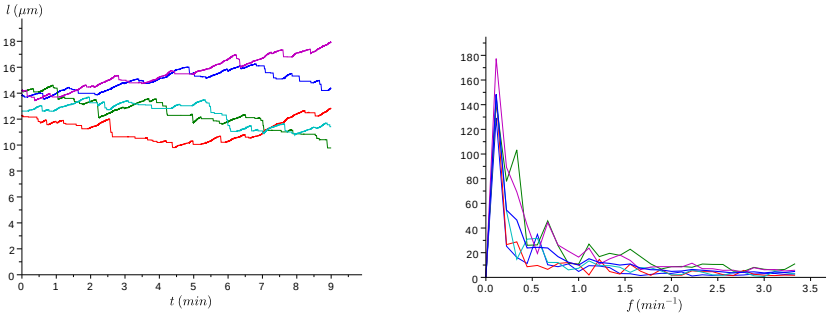

Figure 8. (Left panel) Simulation of $m = 5$ microtubules in the presence of 400 drug molecules, with a total of $\approx 10^5$ tubulin units. The parameter values are as in Figure 4, in addition $r = 0.01$, $q = 0$ and $s = 1$. Here the drug molecules bind to any open site with equal probability. (Right panel) The corresponding absolute Fourier spectra. This simulation suggests a possible action mechanism for the drug S-methyl-D-DM1.

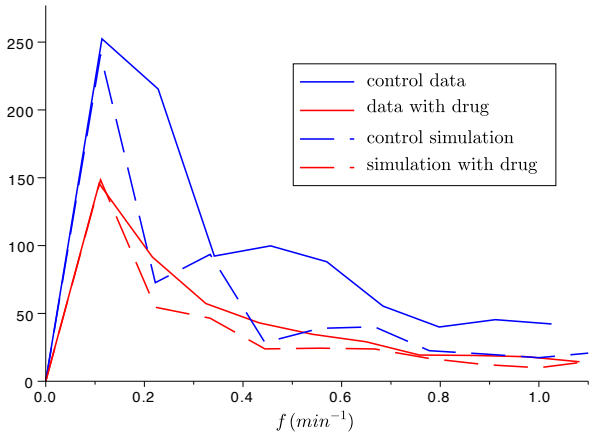

Figure 9. Detail of the average absolute Fourier spectra from Figures 3, 4, 7 and 8. Within the resolution of the frequency grid $\approx 0.11\,min^{-1}$, there is no discernible shift of the position of the peaks.

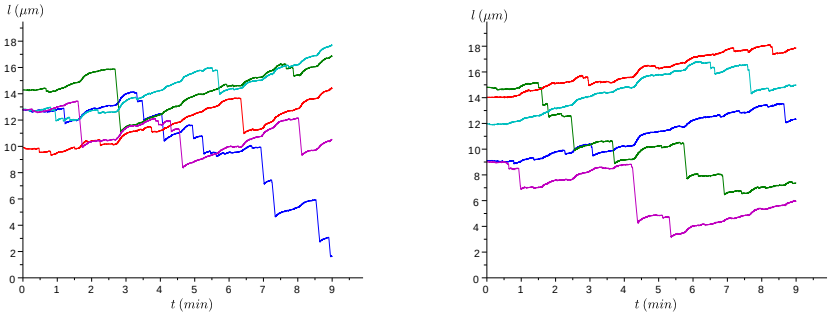

Figure 10. Simulation of $m = 5$ microtubules with a total of $\approx 10^5$ tubulin units in the presence a drug that completely inhibits GTP tubulin hydrolysis. The relevant parameter values are $r = q = 1$ and $s = 0$. The total amount of drug is 20000 (left panel) respectively 40000 (right panel).

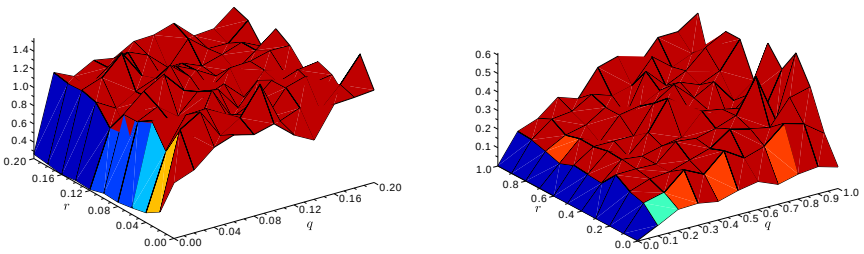

Figure 11. The reduction of microtubule dynamic instability relative to the untreated case as the drug effects vary. Shown are the relative peak heights of the averaged absolute Fourier spectra of 20 microtubules at a concentration of 100 drug molecules for every microtubule. The drug molecules bind either at any open site along the microtubule (left panel) or at the tip only (right panel). The drug does not affect the hydrolysis of bound GTP tubulin ($s = 1$).